J Mol Model (2002) 8:24–32
DOI 10.1007/s00894-001-0064-7

ORIGINAL PAPER

Maciej Baginski · Paolo Polucci · Ippolito Antonini
Sante Martelli

Binding free energy of selected anticancer compounds to DNA – theoretical calculations

Received: 29 August 2001 / Accepted: 31 October 2001 / Published online: 30 January 2002

Abstract Many studies have elucidated structures and thermodynamics of complexes formed by different ligands with DNA. However, in most cases structural and free energy binding studies were not correlated with each other because of the problem of identifying which experimental free energy of binding corresponds to which experimental DNA–ligand structure. In the present work, Poisson–Boltzmann and solvent-accessible surface area methods were used to predict unknown modes of interaction between DNA and three different ligands: mitoxantrone and two pyrimidoacridine derivatives. In parallel, experimental measurements of binding free energy for the studied complexes were performed to compare experimental and calculated values. Our studies showed that the calculated values of free energy are only close to experimental data for some models of interaction between ligands and DNA. Based on this correlation, the most likely models of DNA–ligand complexes were postulated: (i) mitoxantrone and one derivative of pyrimidoacridine, both with two charged side chains, intercalate from the minor groove of DNA and bind with both chains in this groove; (ii) pyrimidoacridine, with only one side chain, very likely does not intercalate into DNA at all. Additionally, the non-electrostatic and electrostatic parts of the calculated binding free energy for the DNA–ligands studied are discussed.

Keywords Binding free energy · DNA–ligand interaction · Mitoxantrone · Pyrimidoacridines · Intercalation

M. Baginski (✉)
Department of Pharmaceutical Technology and Biochemistry, Faculty of Chemistry, Technical University of Gdansk, Narutowicza St 11/12, 80-952 Gdansk, Poland
e-mail: maciekb@hypnos.chem.pg.gda.pl
Tel.: +48-58-3471993, Fax: +48-58-3471144

P. Polucci · I. Antonini · S. Martelli
Department of Chemical Sciences, University of Camerino, Via S. Agostino 1, 62032 Camerino, Italy

Introduction

Studies of interactions between small ligands and DNA, and particularly studies of DNA–ligand binding free energy, are important in chemotherapy but also in basic science to help to understand DNA–protein and DNA–oligonucleotide modes of interaction. On the other hand, an understanding of energetic factors responsible for DNA–ligand binding would help to design more selective ligands that interact with DNA.

Many such small ligands are established anticancer drugs or potent anticancer compounds. These molecules are usually believed to be groove binders or intercalators into DNA. [1, 2, 3, 4] Some recent studies also report structures in which ligands interact with unusual G-quadruplex DNA structures. [5, 6, 7, 8] However, the mode of DNA binding for many anticancer compounds is still not clear. It is widely accepted that DNA intercalation or groove binding is a necessary, but not sufficient, step responsible for antitumor activity of these compounds. [3] Nevertheless, the mode of DNA–drug binding (intercalation or groove binding) may be important for subsequent steps (e.g. inhibition of various DNA binding proteins) and eventually for anticancer activity of these drugs. This may also be valid for compounds that can be activated in vivo, since their initial binding mode can determine the location of chemical bonds between ligand and DNA.

Many studies have elucidated structures of complexes formed by anticancer compounds with DNA. Unfortunately, X-ray or NMR structures are available only for a limited number of compounds. [9, 10, 11] On the other hand, a substantial number of experimental free energy studies have been performed for many ligands interacting with calf thymus DNA (CT-DNA) or polynucleotides. [12, 13, 14, 15, 16, 17] Binding studies indicated the relative binding affinity of different ligands to DNA as well as ligand binding specificity for certain DNA base sequences. These experimental thermodynamic studies, supported by theoretical concepts of polyelectrolyte effects and non-electrostatic effects, posed questions

about different components of the DNA–ligand binding free energy. Such a division of binding free energy into enthalpic and entropic or alternatively electrostatic and non-electrostatic contributions is helpful in understanding which structural elements and molecular properties of ligands and DNA are important for binding. However, in most cases structural and free energy binding studies were not correlated with each other. This is because of problems with identifying which experimental free energy of binding corresponds to which experimental DNA–ligand structure. Usually, experimental free energies of DNA–ligand binding are determined for calf thymus DNA and, on the other hand, experimental molecular structures of the complexes formed (solved by X-ray or NMR methods) are determined for short fragments of DNA. In both cases, the sequences and molecular structures of the complexes (position of ligand and its side chain location within DNA) can be different.

To understand DNA–ligand interactions on the molecular level, computational chemistry methods, as a kind of extension of the experimental approach, have been applied over the last 10–15 years. [18, 19, 20, 21] Most of these theoretical studies used molecular dynamics or, to a lesser extent, other computational chemistry methods to predict structures of DNA–ligand complexes. [22, 23, 24, 25, 26] Some of them applied perturbation free energy or thermodynamic integration molecular dynamics methods to study the relative affinities of similar ligands to DNA or the same ligand to different DNA base sequences. [27, 28, 29, 30] Recently, a new methodology based on Poisson–Boltzmann (PB) equations and solvent-accessible surface area (SASA) methods was used successfully to calculate the free energy of DNA–ligand interactions. [31, 32, 33, 34, 35, 36] This methodology is computationally not very demanding and can reproduce experimental binding free energies obtained for complexes between anthracyclines and DNA quite well. [35]

In the present work, the same PB–SASA methodology was used as a predictive tool to study DNA–ligand modes of interaction. Three compounds with potent anticancer activities: mitoxantrone, [37, 38] and two pyrimidoacridine-derivatives [39] (Fig. 1) were selected for the current project. Pyrimidoacridines are new anticancer compounds that exhibit high cytotoxic activity against multidrug-resistant cell lines. The experimental molecular structure of complexes formed between these molecules and DNA has never been reported. However, by analogy to other compounds with polyaromatic ring systems, one may assume (as a hypothesis) that these molecules interact with DNA by intercalation. In order to determine the most likely model of interaction between the compounds studied and DNA: (i) the binding free energy was measured experimentally for each molecule interacting with CT-DNA, (ii) in parallel, binding free energies were calculated by the PB–SASA methods for different topological models of DNA–ligand complexes. A comparison of the experimental free energy data with calculated values for the different intercalation models enabled us to propose the most likely mode of interaction of each studied compound with DNA.

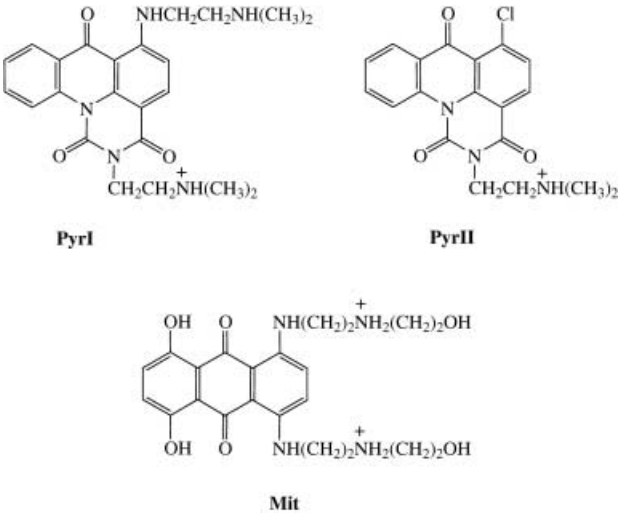

Fig. 1 The structure of studied ligands intercalating into DNA: (Mit) mitoxantrone, (PyrI) 2-[2-(Dimethylamino)ethyl]-6-[2-(dimethylamino)ethylamino]pyrimido[5,6,1-*de*]acridine-1,3,7-trione, (PyrII) 6-Chloro-2-[2-(dimethylamino)ethyl]pyrimido [5,6,1-*de*]acridine-1,3,7-trione

Theory and methods

Binding free energy – measurements

The DNA–ligand binding constants were obtained by fluorescence titration methods. The details of the fluorometric assays have been described previously. [40, 41, 42, 43] The apparent K_{app} ligand binding constant values were determined using a competitive fluorometric ethidium displacement method that has been used extensively for other DNA–binding ligands, particularly intercalators. [40, 42, 43, 44] We only mention here that, in order to remove the absorption spectrum of the intercalator, the fluorescence of that compound was measured at different concentration in the buffer. Recorded values were next removed from the values of fluorescence obtained for the complex DNA–ethidium+compound tested. The C_{50} values are defined as the ligand concentrations that reduce the fluorescence of the DNA-bound ethidium by 50%, and are reported as the mean from three determinations. Apparent equilibrium binding constants K_{app} were calculated from the C_{50} values (in μM) using: $K_{app}=(1.0/C_{50})\times K_{ethidium}$, and with a value of $K_{ethidium}=2.5\times10^6$ M^{-1} for ethidium bromide at 293 K. [44] The C_{50} values for ethidium displacement from CT-DNA were determined using aqueous buffer (10 mM Na_2HPO_4, 10 mM NaH_2PO_4, 1 mM EDTA, pH 7.0) containing 1.0 μM ethidium bromide and 1.35 μM CT-DNA. [40, 42, 45] The total sodium cation concentration in this case was 15 mM.

All measurements were made in 10-mm quartz cuvettes at 20 °C using a Perkin-Elmer LS5 instrument (exci-

tation at 525 nm; emission at 600 nm) following serial addition of aliquots of a stock drug solution (~5 mM in DMSO).

Binding free energy – calculations

Molecular models

To build a model of a DNA–ligand molecular complex, the DNA decamer (5′-d(CpGpApTpCpGpApTpCpG)-3′) was constructed using InsightII (v.95) (MSI, San Diego, Calif.) and in part the X-ray crystallographic data of the DNA–anthracycline intercalation complex. [46] The choice of this particular model of DNA for calculations was based on two rationales: (i) there is evidence that the molecules studied have slightly higher binding affinities to the CG DNA base sequences (mitoxantrone, [47] pyrimidoacridines – our unpublished data) and that the CG sequence forms an intercalation cleft in our DNA model, (ii) the same DNA decamer structure was used previously to study the binding free energy of the DNA–anthracycline intercalation complex and the value of DNA conformational free energy change (i.e. free energy of DNA unwinding) for this DNA model is already known. [35] In the model of DNA studied, the intercalation cavity is located between the central CG bases.

The structures of three molecules were constructed using the Builder module within the InsightII program (MSI, San Diego, Calif.). Protonated forms of molecules were built with hydrogen atoms located at nitrogen atoms of *N*-dimethylamine groups in pyrimidoacridines and at nitrogen atom of *N*-2-hydroxyethyl group in mitoxantrone (Fig. 1). The initial structures were then optimized using the Discover program built into the InsightII packet.

To test different modes of DNA–ligand interactions, several topologically different models of DNA–ligand complex were built for each ligand. These models assume different locations of the ligand's ring system as well as the positions of the side chains. In the case of mitoxantrone, six models of the complex were constructed: (i) mitoxantrone intercalated from the minor groove with both side chains present in this groove in two different orientations: (down, up) – model MitminA, (up, down) – model MitminB, (ii) mitoxantrone intercalated from the major groove with both side chains present in this groove in two different orientations: (down, up) – model MitmajA, (up, down) – model MitmajB, (iii) mitoxantrone placed in the intercalation cavity in such a way that one side chain is present in the minor groove and another one is present in the major groove: the ring C with side chains is close to 3′-5′ DNA strand – model MitintA, the ring C with side chains is close to 5′-3′ DNA strand – model MitintB.

In the case of pyrimidoacridine I (PyrI), which has two side chains similarly to mitoxantrone, six models were built: (i) PyrI intercalated from the minor groove with two locations of ring system (normal and rotated of 180° around the long axis of the ring system) having in both cases the same orientation of the side chains – models PyrIminA, PyrIminB, (ii) PyrI intercalated from the major groove with two locations of ring system (normal and rotated of 180° around the long axis of the ring system) having in both cases the same orientation of the side chains – models PyrImajA, PyrImajB, (iii) PyrI placed in the intercalation cavity in such a way that one side chain is present in the minor groove and another one is present in the major groove: two rings with the side chains are close to 3′-5′ DNA strand – model PyrIintA, the rings with the side chains are close to 5′-3′ DNA strand – model PyrIintB. Since the PyrI ring system is asymmetric, it was necessary to consider normal and upside-down positions of these rings in models (i) and (ii). On the other hand, the PyrI ring system is rather bulky, unlike other intercalators with two side chains, therefore, only one location of the two side chains in DNA grooves was possible and worth studying.

In the case of the molecule PyrII, which has only one side chain and, therefore, may have more conformational freedom in the intercalation cavity, altogether eight models of the DNA–ligand complex were prepared: (i) PyrII intercalated from the minor groove, for which two locations of the ring system (normal and rotated of 180° around the long axis of the ring system) with two positions of side chain (up and down) for each location of the rings are possible; models PyrIIminA1, PyrIIminA2, PyrIIminB1, PyrIIminB2, (ii) PyrII intercalated from the major groove, with two locations of the ring system (normal and rotated of 180° around the long axis of the ring system) and two of the side chain (up and down) for each location of the rings; models PyrIImajA1, PyrIImajA2, PyrIImajB1, PyrIImajB2.

The initial model of each DNA–ligand complex was constructed by visual inspection with the help of the InsightII program (MSI, San Diego, Calif.). The ligands were placed in the central part of the intercalation cavity to avoid short distance van der Waals contacts. Such structures were then optimized using the Charmm force field [48] within Quanta97 (MSI, San Diego, Calif.). All molecular parameters and atomic charges were taken from the set of Charmm force field parameters. During the optimization process, 500 steps of the steepest descent and 1,000 steps of the conjugated gradient algorithm were used. The coordinates of the DNA molecule during the optimization process were fixed. Optimized structures were subsequently used in short molecular dynamics (MD) simulations in vacuum to find the best location of the ligand inside the intercalation cleft. The Charmm force field [48] was used for the MD run. During the simulation the DNA structure was frozen and only the ligands could move. The MD protocol contained a heating part (up to 300 K) lasting 2 ps and then an equilibration part lasting 40 ps. An atom-based cutoff of 18 Å was used to truncate the non-bonding van der Waals and electrostatic interactions. To allow a 2-fs time step, covalent bond lengths of non-polar hydrogen atoms were restrained using the Shake algorithm. The NVT ensemble

(constant temperature and volume) was used in the MD simulations with a temperature coupling interval of 1 ps. The final structure of the DNA–ligand complex obtained after the equilibration step was taken as a starting structure for the binding free energy calculation. An exception was made only for the MitminB model since it resembles the model MitminA after molecular dynamic simulation – both side chains were rotated. This means that only one location of the side chains of Mit in the DNA minor groove is preferred. Therefore, the structure of MitminB for the binding free energy calculations was taken from the stage before the MD run but after a short structure optimization.

PB–SASA calculations

The DNA–ligand intercalation can be described hypothetically as a two step process:

$$\mathrm{DNA} \rightarrow \mathrm{DNA}*$$
$$\mathrm{DNA}* + \mathrm{Lig} \rightarrow \mathrm{DNA}*\mathrm{Lig}$$

The first step describes the conformational change of the DNA (i.e., unwinding) that creates the necessary cavity for the intercalator. The second step is a ligand binding to unwind the DNA. The value of the DNA unwinding free energy for the model of DNA studied in the present work has already been estimated for a similar salt concentration, i.e., 15 mM. The previously obtained value of $\Delta G^{\mathrm{aq}}_{\mathrm{conf}}$ =32.2 kcal mol^{-1} [35] was used here directly and the free energy calculations were performed only for the second process given in the above scheme. The free energy of DNA–ligand association in aqueous solution ($\Delta G^{\mathrm{aq}}_{\mathrm{bind}}$) can be divided into polar (electrostatic) (ΔG^{el}) and non-polar (non-electrostatic) (ΔG^{nel}) terms. [49] Within the last few years non-linear Poisson–Boltzmann (NLPB) equations [50, 51, 52, 53, 54, 55] have been shown to provide an accurate description of the electrostatic interactions between DNA and ligands. [31, 32, 33, 35, 36, 56, 57, 58, 59] This approach was used in the present study to calculate electrostatic contributions to the binding free energy, while non-polar contributions were calculated using the SASA method. [60, 61, 62, 63, 64, 65] The thermodynamic cycle corresponding to DNA*–ligand binding is shown in Fig. 2. The solvation free energy in this cycle corresponds to the free energy of transfer from a low dielectric phase (the alkane phase) to aqueous solution. It was faster to calculate the electrostatic contribution to the solvation free energy for the transfer from the alkane phase to aqueous solution rather than from vacuum to water. In the former case, we assume the alkane phase to have a dielectric constant ε=4, which is also equal to the internal dielectric constant for the molecule (see last paragraph in PB–SASA calculations). The finite-difference method was used to solve the NLPB equations. In this case, it was possible to use the method of Green's functions to subtract the self-energy. [66] Additionally, the transfer of a molecule from a phase of ε=4 to a phase of ε=78 justifies the application of a microscopic surface tension coefficient used in SASA methods.

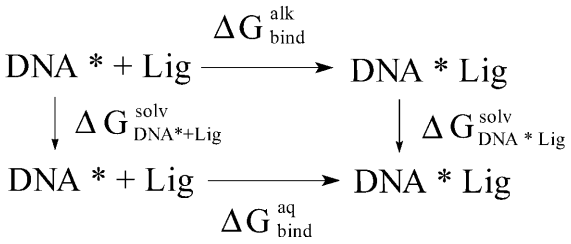

Fig. 2 The thermodynamic cycle of studied DNA–ligand complexes corresponding to the process of ligand intercalation to unwound DNA*

According to the thermodynamic cycle in Fig. 2, the binding free energy of the ligand to DNA* (in this case, it is unwound DNA ready for intercalation) is defined as:

$$\Delta G^{\mathrm{aq}}_{\mathrm{bind}} = \Delta G^{\mathrm{solv}}_{\mathrm{DNA}*\mathrm{Lig}} - \Delta G^{\mathrm{solv}}_{\mathrm{DNA}*+\mathrm{Lig}} + \Delta G^{\mathrm{alk}}_{\mathrm{bind}} \quad (1)$$

and, when one separates electrostatic and non-electrostatic contributions, it can be expressed as:

$$\Delta G^{\mathrm{aq}}_{\mathrm{bind}} = \Delta G^{\mathrm{solv,el}}_{\mathrm{DNA}*\mathrm{Lig}} + \Delta G^{\mathrm{solv,nel}}_{\mathrm{DNA}*\mathrm{Lig}} - \Delta G^{\mathrm{solv,el}}_{\mathrm{DNA}*+\mathrm{Lig}} - \Delta G^{\mathrm{solv,nel}}_{\mathrm{DNA}*+\mathrm{Lig}} + \Delta G^{\mathrm{alk,el}}_{\mathrm{bind}} + \Delta G^{\mathrm{alk,nel}}_{\mathrm{bind}} \quad (2)$$

The electrostatic and non-electrostatic contributions in this equation can be grouped together since the self energy in the NLPB equations cancels out due to the same positioning of the grid for the complex and the substrates. [67] The first two non-electrostatic terms can also be put together. The second non-electrostatic term $\Delta G^{\mathrm{alk,nel}}_{\mathrm{bind}}$ is equal to 0 since there are no conformational changes during binding and the complex formation in low dielectric medium corresponds to transferring the ligand from the non-polar medium to the non-polar interior of DNA* with the same dielectric constant. Thus Eq. (2) can be rewritten as follows:

$$\Delta G^{\mathrm{aq}}_{\mathrm{bind}} = \Delta G^{\mathrm{el}}_{\mathrm{bind}} + \Delta G^{\mathrm{solv,nel}}_{\mathrm{bind}} \quad (3)$$

The first term of Eq. (3) was calculated by the NLPB method and the second term was calculated by the SASA method according to the equation:

$$\Delta G^{\mathrm{solv,nel}}_{\mathrm{bind}} = \gamma \Delta A_{\mathrm{bind}} \quad (4)$$

where ΔA_{bind} is a difference between the solvent-accessible surface area for the complex and the substrates. The coefficient γ=0.050 kcal mol^{-1} Å^{-2} [35, 36, 68, 69] is a microscopic surface tension coefficient relating the solvent-accessible surface area to the free energy of transferring a molecule from an alkane to a water phase. [70] The solvent-accessible areas were obtained in these calculations using a probe radius of 1.4 Å.

All the electrostatic contributions to the DNA–ligand binding free energy were calculated using the UHBD program. [67, 71] Non-linear Poisson–Boltzmann equations

were used. The molecular parameters, i.e., atom charges and van der Waals radii for all atoms of ligands and DNA* were taken from the Charmm force field. The same parameters were used during the initial structure preparations with the Charmm program. In the UHBD calculations each molecule was treated as a low dielectric cavity with ε=4. This dielectric constant was used to account for electronic polarization and dipole fluctuations inside the molecule. The same value was also used previously for DNA. [32, 35] The cavity was defined by the molecular surface obtained using a probe radius of 1.4 Å. The water solvent was treated as a continuum of dielectric constant ε=78. A radius of 2.0 Å was used to exclude monovalent ions from the surface of each molecule. The monovalent ion concentration was kept at the level of c=15 mM Na^+ in all electrostatic calculations – this value corresponds to the experimental monovalent ion concentration at which the binding free energy was obtained. The electrostatic focusing procedure was used for NLPB calculations. [72] First the electrostatic potential was calculated on a cubic lattice of 110×110×110 points. The initial grid mesh size was 1.0 Å. Next, a grid mesh size of 0.5 Å was used. The calculations of the electrostatic free energy contribution for ligand, DNA and DNA–ligand complex were performed for the same position of the cubic lattice. The positions (i.e., Cartesian coordinates) of a ligand and DNA alone were the same as their positions in the complex. The surface boundary smoothing procedure was also employed. [73, 74] Finally, it is worth mentioning that the main source of errors in our DNA–ligand free energy binding calculations by the PB–SASA method does not stem from the variation of molecular parameters in the PB calculation but from uncertainties of DNA–ligand structure of the complex. For example, for randomly chosen structures from the equilibration stage of an MD run, a difference of ±1 kcal mol^{-1} of binding free energy was found for DNA–MitminA complex, which corresponds to roughly 7% of the total value.

Results and discussion

Experimental values of binding free energy

The experimental values of DNA–ligand binding constants and corresponding free energy values are shown in Table 1. The reported values of binding free energy for all three compounds are of the order of –6 to –10 kcal mol^{-1} and are comparable to those of other DNA–ligand complexes. [15] The differences between the compounds are of the order of 1–2 kcal mol^{-1}. The source of these differences may come from the fact that both Mit and PyrI molecules have two side chains with protonated amino groups that can interact with DNA grooves. On the other hand, PyrII has only one such side chain. Therefore, its interaction with DNA can be weaker.

Table 1 The experimental values of DNA–ligand binding free energy. C_{50} – concentration of the compound needed to reduce the DNA–ethidium complex fluorescence by 50%; mean value (±5%) from three determinations. K_{app} – apparent ligand binding constant (see Theory and methods for the definition). ΔG_{bind} – calculated values of binding free energy according to the equation $\Delta G_{bind}=-RT\ln(K_{app})$ for T=293 K

Compound	C_{50} (μM)	$10^{-6}\,K_{app}$ (M^{-1})	ΔG_{bind} (kcal mol^{-1})
Mit	0.053	47.170	–10.3
PyrI	0.580	4.310	–8.9
PyrII	28.600	0.087	–6.6

Calculated values of binding free energy

The calculated values of DNA–ligand binding free energy for mitoxantrone and two derivatives of pyrimidoacridines are presented in Table 2. The binding free energy is dissected according to the approach outlined in the Theory and methods section for electrostatic (ΔG^{el}_{bind}) and non-electrostatic ($\Delta G^{solv,nel}_{bind}$) contributions. The first one was calculated by solving the NLPB equations, the second using the SASA method. The last column in Table 2 additionally reports the total DNA–ligand binding free energy that includes the conformational unwinding of DNA necessary for ligand intercalation. The values from this column can be compared directly with the experimental values of binding free energy presented in Table 1. The only missing contribution in our free energy calculations (last column in Table 2) accounts for the entropy term concerning the reduction of translational and rotational freedom of a ligand and DNA upon binding. An extensive discussion how other entropic terms are implicitly included in our calculations and generally how to treat entropic corrections in calculations of binding free energy between DNA and small ligands is presented in the work of Baginski et al. [35] The estimated value of the translational–rotational entropy contribution for DNA–anthracycline complexes is ca. 4 kcal mol^{-1}. [35] This value is smaller than the ~10–15 kcal mol^{-1} used by others (e.g. [15, 75]) in the parsing scheme of ligand–DNA binding free energy. However, recently similar values to our data were also reported for the entropy cost of protein association. [76] In our case, the ligands – especially Mit and PyrI with two side chains – may be regarded as more flexible than anthracyclines. Therefore, one may assume somewhat higher values than estimated for anthracyclines (i.e., about 6–8 kcal mol^{-1}) as the proper entropy correction. This additional entropy cost is due to loss of conformational chain freedom and was previously estimated to be of the order of ca. 2 kcal mol^{-1} for short chains. [77, 78, 79] Taking into account such an entropy correction, we find that our calculated values of DNA–ligand binding free energy are very close to the experimental data. It should be noted that the values of binding free energy corrected by 6 kcal mol^{-1} for Mit and PyrI and corrected by 4 kcal mol^{-1} for PyrII) are presented in Table 2 in parentheses. In the latter case, the value is the same as for DNA–anthracycline complexes [35] since PyrII and anthracyclines have only one

Table 2 The calculated values of DNA–ligand binding free energy for topologically different complexes of Mit, PyrI, and PyrII with DNA. The electrostatic part was calculated within the PB approach, the non-electrostatic part was calculated using SASA methods. The binding part is the sum of electrostatic and non-electrostatic contributions. Total binding free energy includes additionally free energy of DNA unwinding – the value of 32.2 kcal mol^{-1} taken from Baginski et al. [35] was applied. The values in parentheses present total binding free energy that includes entropic corrections – see the text. All values are given in kcal mol^{-1}

Name of complex	Elec. part ΔG^{el}_{bind}	Non-elec. part $\Delta G^{solv,nel}_{bind}$	Binding ΔG^{aq}_{bind}	Total ΔG^{aq}_{bind}
MitminA	–0.8	–48.2	–49.0	–16.8(–10.8)
MitminB	–0.3	–39.7	–40.0	–7.8(–1.8)
MitmajA	–2.2	–36.9	–39.1	–6.9(–0.9)
MitmajB	+4.2	–37.9	–33.7	–1.5(+4.5)
MitintA	–2.5	–40.5	–43.0	–10.8(–4.8)
MitintB	–2.2	–41.8	–44.0	–11.8(–5.8)
PyrIminA	+0.9	–47.2	–46.3	–14.1(–8.1)
PyrIminB	+0.3	–46.8	–46.5	–14.3(–8.3)
PyrImajA	–2.1	–36.7	–38.8	–6.6(–0.6)
PyrImajB	–3.8	–35.6	–39.4	–7.2(–1.2)
PyrIintA	+2.2	–41.4	–39.2	–7.0(–1.0)
PyrIintB	–6.2	–41.7	–47.9	–15.7(–9.7)
PyrIIminA1	+2.8	–39.7	–36.9	–4.7(–0.7)
PyrIIminA2	+2.3	–38.2	–35.9	–3.7(+0.3)
PyrIIminB1	+2.8	–38.7	–35.9	–3.7(+0.3)
PyrIIminB2	+1.3	–38.0	–36.7	–4.5(–0.5)
PyrIImajA1	–0.3	–30.2	–30.5	+1.7(+5.7)
PyrIImajA2	+4.1	–29.9	–25.8	+6.4(+10.4)
PyrIImajB1	+0.4	–30.8	–30.4	+1.8(+5.8)
PyrIImajB2	+2.1	–35.3	–33.2	–1.0(+3.0)

substituent. Nevertheless, we do not claim that our calculations can reproduce quantitatively absolute values of binding free energy. In the best case, one may regard our calculated values as semiquantitative. However, as demonstrated previously, [35] experimental relative values of binding free energy for DNA–anthracycline complexes were reproduced fairly well.

The free energy calculations were performed for several topologically different models of intercalation for each ligand. In case of Mit only the binding free energy value corresponding to intercalation from the minor groove is close to the experimental value. Actually, the model MitminA can be regarded as the most probable for intercalation (Fig. 3a). The location of MitminA side chains in the minor groove is rather natural and fits well to the DNA turn. On the contrary, a reversed position of the side chains in the MitminB model substantially increases the binding free energy. This suggests that only one location of side chains in the minor groove is preferred. The predicted values of binding free energy for the models Mitmaj (intercalation from the major groove) and Mitint (intercalation with one chain in the minor groove and the second chain in the major groove) are rather far from the experimental value. This means that such modes of interaction between Mit and DNA are very unlikely.

The calculated values of binding free energy between PyrI and DNA are close to experimental data only in the case of models PyrIminA, PyrIminB and PyrIintB. The first two models correspond to ligand intercalation from the minor groove and are similar to the intercalation models predicted for mitoxantrone (Fig. 3b). One should also consider the model PyrIintB (Fig. 3c) as very likely from the thermodynamic point of view. The value of the binding free energy for this model is even lower than that obtained experimentally (Table 2). Nevertheless, the PyrIintB model of intercalation with one chain in the minor groove and the second in the major groove should be considered with some caution. The bulky ring system and two side chains of the PyrI molecule may have some problems to intercalate just from one side, and therefore the intercalation mode with one chain in the minor and one in the major groove can be a kind of alternative intercalation structure without conformational crowding. On the other hand, it is very rare situation and, to the best of our knowledge, there is only one reported structure of a DNA–ligand complex where the ligand has two substituents attached to the ring system and each substituent is placed in a different DNA groove. [80]

The calculated values of binding free energy for the DNA–PyrII complex differ substantially from experimental data regardless of which intercalation model is considered. Taking into account a fairly good agreement between the experimental and calculated values of binding free energy for anthracyclines [35] and in the present work for Mit and PyrI, it is reasonable to reject the assumed models of intercalation for PyrII. These models do not reproduce even semiquantitatively the experimental binding free energy. Since the free energy calculations were performed for many different models of intercalations it looks as if PyrII does not intercalate into DNA. This means that intercalation as the assumed mode of interaction between DNA and PyrII was not correct and one should consider other modes of interaction, e.g., groove-binding. Such an alternative binding may also be supported by biological cytotoxic data. [39] The compound PyrII is much less cytotoxic than PyrI (i.e., the EC_{50} for PyrII is two orders of magnitude higher than that for PyrI). [39] Such a difference in the cytotoxic activity may be explained by a different interaction of the molecules studied with DNA. Of course the cytotoxic data come from in vitro experiments in tissue culture and some additional effects such as metabolic activation or cellular uptake may be responsible for the di-

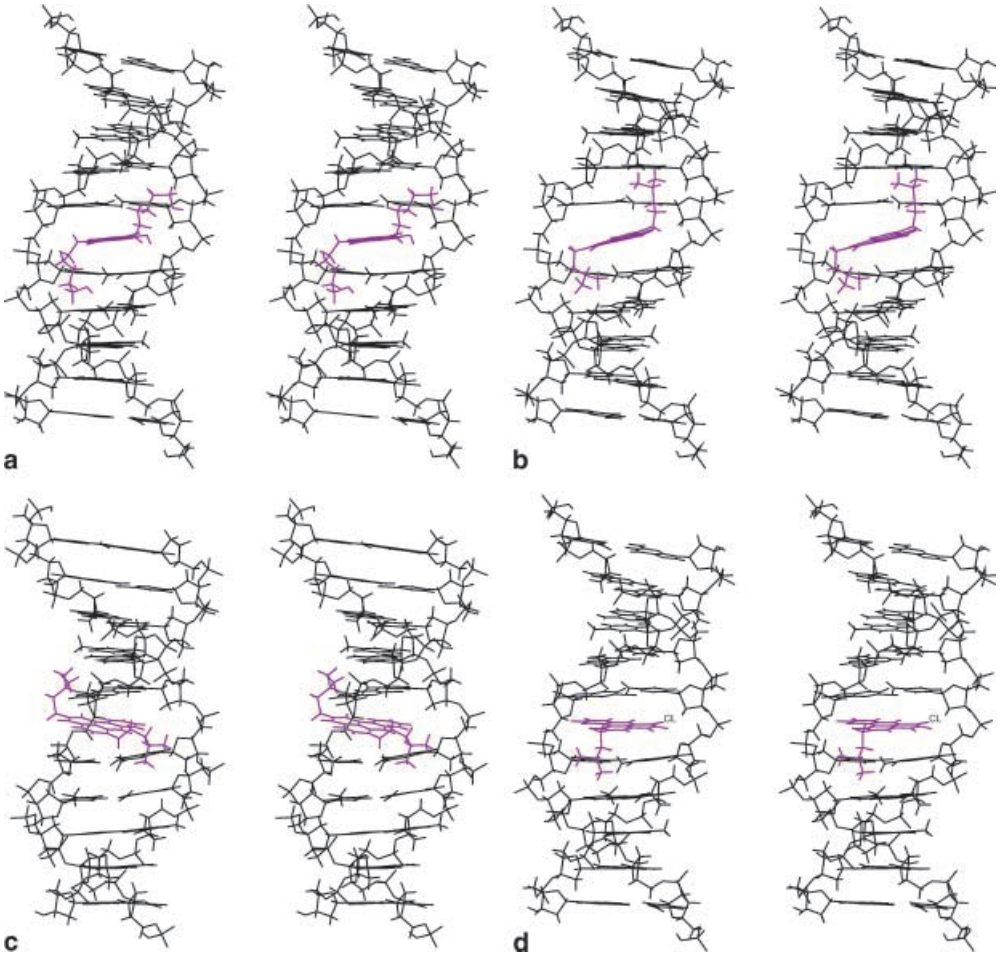

Fig. 3a–d Structure of selected models of DNA–ligand complexes (stereoview): **a** model MitminA – the most likely structure of DNA–Mit complex, **b** model PyrIminB – the most likely structure of DNA–PyrI complex, **c** model PyrIintB – thermodynamically allowed but kinetically rather difficult to obtain structure of DNA–PyrI complex with each side chain in a different DNA groove, **d** model PyrIIminA1 – rather unlikely from steric reasons structure of DNA–PyrII complex. DNA is *black* and ligands are *blue*. See text and Table 2 for further description

verse cytotoxic activities. Nevertheless, altogether, binding studies, calculation of free energy, and cytotoxic data strongly support the hypothesis that PyrII interacts with DNA in a different way than PyrI or Mit. Since the experimental binding free energy of PyrII is higher than that of PyrI, one may suspect that PyrII binds only to a minor or major DNA groove. From the molecular point of view it is also worth mentioning that intercalation of PyrII into DNA may be not possible because of the size of the chlorine atom. The chlorine atom may act in this case as a molecular obstacle preventing intercalation. All intercalation models of PyrII assume that the side chain is present in one of the DNA grooves. This means that the chlorine atom (Figs. 1 and 3d) replacing the second side chain is present either partly in the intercalation cavity or in the opposite groove. Since the chlorine atom is not only bulky but also carries a negative net charge, its location in the intercalation cavity or groove is thermodynamically very unfavorable. The negative electrostatic potential of DNA in both grooves [35, 81] supports this idea because the chlorine atom will be repelled electrostatically from the grooves.

Finally, it is worth discussing the different terms of the DNA–ligand binding free energy. In all cases, the electrostatic contribution ΔG^{el}_{bind} (Table 2) to the binding free energy is around zero (both positive or negative) which was also found for anthracyclines [35] and phenylphenanthridine [32] within the PB approach. The electrostatic contribution for the predicted models of intercalation MitminA and MitminB is slightly negative. This means that two protonated chains of Mit prefer to stay in the DNA groove, rather than in bulk solvent. Since each Mit chain carries not only one charged group but also a polar hydroxyl group, its electrostatic interactions with DNA may quite well replace the solvation of the DNA groove by ions. The release of ions from the DNA groove after binding can be compensated in this case by polar and charged groups of Mit placed in the groove upon binding. The situation is different when PyrI binds to DNA. PyrI has only one charged group in the side chain and no other polar groups. Additionally, this charged group is quite bulky. The release of ions from the DNA groove by this group upon binding is not compensated by electrostatic interactions with the side chain of PyrI.

It is also worth discussing all other cases for MitI and PyrI where the non-polar contribution is negative but the total free energy is higher than those for the most favorable complexes. The negative electrostatic contribution in these models is due to very specific either intra- or in-

termolecular hydrogen bonds formed by ligands. However, this more negative contribution is not compensated by the non-electrostatic contribution, which is always higher in these cases. The source of increased non-electrostatic contribution to the binding free energy stems from the fact that the ligand forming these specific hydrogen bonds does not bind tightly to DNA. In this case, the change of surface-accessible surface area of molecules upon binding is not as large and non-electrostatic interactions are not emphasized as strongly.

Comparing different contributions to the binding free energy in Table 2, one can say that the driving forces for ligand binding and eventually intercalation into DNA are non-polar interactions $\Delta G_{\text{bind}}^{\text{solv,nel}}$ resulting from the burial of interfacial surface area of both DNA and ligand (column III in Table 2). This non-polar contribution to the binding free energy is always highly negative because of the release of water molecules from the surface of DNA and ligand. The release of water molecules is hydrophobic in nature since, according to the thermodynamic cycle in Fig. 2 and Eq. (2), it corresponds to the situation when interacting molecules are not charged. It is worth underlining that negative values of non-electrostatic contributions ("hydrophobic" effects) to the binding free energy as the driving force of the whole binding process were found for DNA–protein [36, 82, 83, 84] and other DNA–ligand [35, 85, 86] complexes.

Interestingly, different contributions to DNA–ligand binding free energy have recently been presented by others. [15, 75] In these studies the binding free energy is also divided into conformational, entropic, hydrophobic (non-electrostatic), polyelectrolyte (electrostatic) and additionally noncovalent (hydrogen bonds) contributions. Estimation of different contributions to the binding free energy for DNA–groove binder Hoechst 33258 works quite well and the final binding energy is very close to the experimental value. [15] However, when one tries to add the estimated contributions to the binding free energy for DNA intercalators, e.g., daunorubicin or doxorubicin (given in the same work [15]) the final value of the DNA–ligand binding free energy is substantially different from the experimental value and may even take positive values. This is especially true when one takes into account the energy contribution necessary for conformational change of the DNA (unwinding). Comparing our calculated contributions to the binding free energy (current work) and previous estimates for anthracyclines, [35] it appears that values estimated by Chaires's group [15, 75] are less negative than those obtained by us for hydrophobic interactions. On the contrary, our estimation of the DNA-unwinding free energy, [35] which takes into account both electrostatic and non-electrostatic contributions, is higher than that discussed in references [15, 75]. Also the values of entropic changes due to loss of translational and rotational freedom upon binding differ from article to article. In our case values from 4 to 6 kcal mol^{-1} are used and in references [15, 75] a value of 15 kcal mol^{-1} was used. Clearly, further studies are necessary to determine the most likely contributions to the binding free energy of DNA–ligand complexes when the ligand intercalates into DNA.

Conclusion

In this work experimental as well as calculated values of binding free energies of selected ligands (i.e., mitoxantrone and pyrimidoacridines) to DNA were obtained. Since the experimental structures of the DNA–ligand complexes studied were not available, the PB-SASA methods were used as a predictive tool to study the mode of DNA–ligand interactions. This theoretical approach was justified by a previous study of DNA–small ligand and DNA–protein binding free energies. Therefore, comparison of calculated values with experimental data for different models of DNA–ligand complexes enables us to point out the most likely structures. It was found that mitoxantrone and one derivative of pyrimidoacridine (PyrI), both with two side chains, intercalate into DNA from the minor groove. In both cases, the side chains stay in the minor groove of DNA. On the other hand, we hypothesize that another derivative of pyrimidoacridine (PyrII), with only one side chain, does not intercalate into DNA. Based on the large discrepancy between the calculated and experimental binding free energies we postulate a groove-binding mode of PyrII interaction with DNA. The different mode of interaction with DNA between Mit or PyrI and PyrII is also supported by substantial difference in the biological activity between these compounds.

Additionally, our studies showed that the binding of the studied ligands with DNA is driven by non-electrostatic interactions. This finding is in agreement with recent results obtained for other molecules (small ligands and proteins) interacting with DNA.

In summary, the successful application of the PB-SASA method to our particular problem suggests that this methodology is a potent predictive tool to study, at least in a semiquantitative way, binding free energies of DNA–ligand complexes even in cases when the structure of these complexes is not known. In these cases, a comparison of experimental and calculated free energy values enables us to suggest the most likely mode of DNA–ligand interaction.

Acknowledgements We acknowledge the financial support from University of Camerino (Italy) as well as Technical University of Gdansk (Poland) internal grants. Additionally, M.B. would like to thank the Computational Center TASK (Gdansk, Poland) for granting CPU time.

References

1. Geierstanger BH, Wemmer DE (1995) Annu Rev Biophys Biomol Struc 24:463
2. Neidle S (1997) Biopolymers 44:105
3. Denny WA (1989) Anti Cancer Drug Des 4:241
4. Neidle S, Abraham Z (1984) CRC Crit Rev Biochem 17:73

5. Fedoroff OY, Salazar M, Han HY, Chemeris VV, Kerwin SM, Hurley LH (1998) Biochemistry 37:12367
6. Perry PJ, Gowan SM, Read MA, Kelland LR, Neidle S (1999) Anti Cancer Drug Des 14:373
7. Mergny JL, Mailliet P, Lavelle F, Riou JF, Laoui A, Helene C (1999) Anti Cancer Drug Des 14:327
8. Read MA, Neidle S (2000) Biochemistry 39:13422
9. Neidle S, Nunn CM (1998) Nat Prod Rep 15:1
10. Berman HM, Olson WK, Beveridge DL, Westbrook J, Gelbin, A, Demeny T, Hsieh SH, Srinivasan AR, Schneider B (1992) Biophys J 63:751
11. Berman HM, Gelbin A, Westbrook J (1996) Prog Biophys Mol Biol 66:255
12. Marky LA, Snyder JG, Remeta DP, Breslauer KJ (1983) J Biomol Struct Dyn 1:487
13. Breslauer KJ, Remeta DP, Chou W-Y, Ferrante R, Curry J, Zaunczkowski D, Snyder JG, Marky LA (1987) Proc Natl Acad Sci USA 84:8922
14. Chaires JB (1996) Anti Cancer Drug Des 11:569
15. Chaires JB (1997) Biopolymers 44:201
16. Chaires JB, Satyanarayana S, Suh D, Fokt I, Przewloka T, Priebe W (1996) Biochemistry 35:2047
17. Schwaller MA, Dodin G, Aubard J (1991) Biopolymers 31:519
18. Kollman PA, Weiner S, Seibel G, Lybrand T, Singh UC, Caldwell J, Rao SN (1986) Ann NY Acad Sci 482:234
19. Veal JM, Wilson WD (1991) J Biomol Struct Dyn 8:1119
20. Neidle S, Jenkins TC (1991) Methods Enzymol 203:433
21. Herzyk P, Neidle S, Goodfellow JM (1992) J Biomol Struct Dyn 10:97
22. Creighton S, Rudolph B, Lybrand T, Singh UC, Shafer R, Brown S, Kollman P, Case DA, Andrea T (1989) J Biomol Struct Dyn 6:929
23. Boehncke K, Nonella M, Schulten K, Wang AH (1991) Biochemistry 30:5465
24. Searle MS, Bicknell W (1992) Eur J Biochem 205:45
25. Remias MG, Lee CS, Haworth IS (1995) J Biomol Struct Dyn 12:911
26. Jayaram B, Aneja N, Rajasekaran E, Arora V, Das A, Ranganathan V, Gupta V (1994) J Sci Ind Res India 53:88
27. Gago F, Richards WG (1990) Mol Pharmacol 37:341
28. Cieplak P, Rao SN, Grootenhuis PD, Kollman PA (1990) Biopolymers 29:717
29. Shi YY, Zhao HM, Wang CX (1993) Int J Biol Macromol 15:247
30. Singh SB, Ajay, Wemmer DE, Kollman PA (1994) Proc Natl Acad Sci USA 91:7673
31. Zacharias M, Luty BA, Davis ME, McCammon JA (1992) Biophys J 63:1280
32. Misra VK, Honig B (1995) Proc Natl Acad Sci USA 92:4691
33. Misra VK, Sharp KA, Friedman RA, Honig B (1994) J Mol Biol 238:245
34. Areas EPG, Pascutti PG, Schreier S, Mundim KC, Bisch PM (1995) J Phys Chem 99:14885
35. Baginski M, Fogolari F, Briggs JM (1997) J Mol Biol 274:253
36. Misra VK, Hecht JL, Yang AS, Honig B (1998) Biophys J 75:2262
37. Johnson RK, Zee-Cheng RK, Lee WW, Acton, EM, Henry DW, Cheng CC (1979) Cancer Treat Rep 63:425
38. Murdock KC, Child RG, Fabio PF, Angier RB, Wallace RE, Durr FE, Citarella RV (1979) J Med Chem 22:1024
39. Antonini I, Cola D, Polucci P, Bontemps-Gracz M, Borowski E, Martelli S (1995) J Med Chem 38:3282
40. Morgan AR, Lee JS, Pulleyblank DE, Murray NL, Evans DH (1979) Nucleic Acids Res 7:547
41. Chen Q, Deady LW, Baguley BC, Denny WA (1994) J Med Chem 37:593
42. McConnaughie AW, Jenkins TC (1995) J Med Chem 38:3488
43. Antonini I, Polucci P, Cola D, Bontemps Gracz M, Pescalli N, Menta E, Martelli S (1996) Anti Cancer Drug Des 11:339
44. Le Pecq JB, Paoletti C (1967) J Mol Biol 27:87
45. Baguley BC, Denny WA, Atwell GJ, Cain BF (1981) J Med Chem 24:170
46. Moore MH, Hunter WN, Langlois D'Estaintot B, Kennard O (1989) J Mol Biol 206:693
47. Panousis C, Phillips DR (1994) Nucleic Acids Res 22:1342
48. Brooks BR, Bruccoleri RE, Olafson BD, States DJ, Swaminathan S, Karplus M (1983) J Comput Chem 4:187
49. Honig B, Sharp K, Yang AS (1993) J Phys Chem 97:1101
50. Chen SWW, Honig B (1997) J Phys Chem B 101:9113
51. Honig B, Nicholls A (1995) Science 268:1144
52. Sharp KA, Honig B (1990) Annu Rev Biophys Biophys Chem 19:301
53. Madura JD, Davis ME, Gilson MK, Wade RC, Luty BA, McCammon JA (1994) Biological applications of electrostatic calculations and brownian dynamics simulations. In: Lipkowitz KB, Boyd DB (eds) Reviews in computational chemistry. VCH, New York, pp 229–267
54. Davis ME, McCammon JA (1990) Chem Rev 90:509
55. Gilson MK, Honig B (1988) Proteins 4:7
56. Gallagher K, Sharp K (1998) Biophys J 75:769
57. Fogolari F, Elcock AH, Esposito G, Viglino P, Briggs JM, McCammon JA (1997) J Mol Biol 267:368
58. Sharp KA, Friedman RA, Misra VK, Hecht JL, Honig B (1995) Biopolymers 36:245
59. Misra VK, Hecht JL, Sharp KA, Friedman RA, Honig B (1994) J Mol Biol 238:264
60. Cramer CJ, Truhlar DG (1995) Continuum solvation models: classical and quantum mechanical implementation. In: Lipkowitz KB, Boyd DB (eds) Reviews in computational chemistry, vol 6. VCH, New York, pp 1–72
61. Sitkoff D, Sharp KA, Honig B (1994) Biophys Chem 51:397
62. Hermann RB (1972) J Phys Chem 76:2754
63. Tunon I, Silla E, Pascualahuir JL (1992) Protein Eng 5:715
64. Ooi T, Oobatake M, Nemethy G, Scheraga HA (1987) Proc Natl Acad Sci USA 84:3086
65. Rashin AA, Bukatin MA (1994) Biophys Chem 51:167
66. Luty BA, Davis ME, McCammon JA (1992) J Comput Chem 13:768
67. Madura JD, Briggs JM, Wade RC, Davis ME, Luty BA, Ilin A, Antosiewicz J, Gilson MK, Bagheri B, Scott LR, McCammon JA (1995) Comput Phys Commun 91:57
68. Friedman RA, Honig B (1995) Biophys J 69:1528
69. Froloff N, Windemuth A, Honig B (1997) Protein Sci 6:1293
70. Sharp KA, Nicholls A, Friedman R, Honig B (1991) Biochemistry 30:9686
71. Davis ME, Madura JD, Luty BA, McCammon JA (1991) Comput Phys Commun 62:187
72. Gilson MK, Sharp KA, Honig BH (1987) J Comput Chem 9:327
73. Davis ME, McCammon JA (1991) J Comput Chem 12:909
74. Mohan V, Davis ME, McCammon JA, Pettitt BM (1992) J Phys Chem 96:6428
75. Ren JS, Jenkins TC, Chaires JB (2000) Biochemistry 39:8439
76. Tamura A, Privalov PL (1997) J Mol Biol 273:1048
77. Collet O, Premilat S (1993) Macromolecules 26:6076
78. Sternberg MJE, Chickos JS (1994) Protein Eng 7:149
79. Koehl P, Delarue M (1994) J Mol Biol 239:249
80. Hansen M, Hurley L (1995) J Am Chem Soc 117:2421
81. Jayaram B, Sharp KA, Honig B (1989) Biopolymers 28:975
82. Spolar RS, Record MT (1994) Science 263:777
83. Lundback T, Cairns C, Gustafsson J, Carlstedt-Duke J, Hard T (1993) Biochemistry 32:5074
84. Ha J, Spolar RS, Record MT (1989) J Mol Biol 209:801
85. Ding W, Ellestad GA (1991) J Am Chem Soc 113:6617
86. Boger DL, Invergo BJ, Coleman RS, Zarrinmayeh H, Kitos PA, Collins-Thompson S, Leong T, McLaughlin LW (1990) Chem Biol Interact 73:29